

1 1. Introduction

2 We have studied the concept, implementation and
 3 performance of a novel deep sea neutrino experiment
 4 [1] which has the main goal to measure the mixing
 5 angle θ_{13} with high precision. The CNGS [2] neutrino
 6 beam, which is currently under construction, could be
 7 converted with modest effort (no civil engineering) to
 8 a quasi-monoenergetic off-axis neutrino beam,
 9 delivering ν_μ of $E_\nu \approx 0.8$ GeV from CERN to the
 10 Gulf of Taranto (C2GT) (radial distance from CNGS
 11 Beam axis: 44 km). The experimental concept of
 12 C2GT consists of a planar Cherenkov underwater
 13 detector, operated at a depth of ~ 1000 m, and at
 14 baselines around 1200 km. A 600 km long deep see
 15 trench with minimal depth of 1000 m allows to
 16 displace the detector in order to assess baselines from
 17 1100 – 1700 km.

18 Under certain assumptions, neutrino oscillations at
 19 large (planetary) distances can be described by only 3
 20 parameters: θ_{23} , $\Delta m_{23}^2 \approx \Delta m_{13}^2$, θ_{13}

21 In a first phase the experiment measures $\nu_\mu \leftrightarrow \nu_\tau$
 22 oscillations at 3 different baselines L and determines
 23 $\sin^2 \theta_{23}$ and Δm_{23}^2 from

$$24 \quad P(\nu_\mu \leftrightarrow \nu_\tau) \cong \cos^4 \theta_{13} \sin^2 2\theta_{23} \sin^2 \left(\frac{1.27 \Delta m_{23}^2 L}{E_\nu} \right)$$

25 As the neutrino energy is below the τ production
 26 threshold, a ν_μ disappearance experiment is
 27 performed. At a certain baseline L^* , depending on the
 28 precise value of Δm_{23}^2 , the term
 29 $\sin^2 \left(1.27 \Delta m_{23}^2 L^* / E_\nu \right)$ will have the value one and
 30 the experiment will provide maximum sensitivity for
 31 the measurement of $\nu_\mu \leftrightarrow \nu_e$ oscillations, which allow
 32 to extract $\sin^2 \theta_{13}$ from

$$33 \quad P(\nu_\mu \leftrightarrow \nu_e) \cong \sin^2 \theta_{23} \sin^2 \theta_{13} \sin^2 \left(\frac{1.27 \Delta m_{23}^2 L^*}{E_\nu} \right)$$

34 After running for 1+1+5 years (at baselines L_1 , L_2 ,
 35 L^*) the expected precision on $\sin^2 \theta_{23}$ and Δm_{23}^2
 36 are 8% and 1%, respectively. The experiment would
 37 allow to improve the current upper limit of $\sin^2 \theta_{13}$
 38 of 0.05 by a factor 30 or could establish a non-zero
 39 value of $\sin^2 \theta_{13}$ down to 0.0039.

40 The detector consists of a grid of $\sim 300 \times 300$ m²
 41 size, subdivided in mechanical modules of 10×10

42 m² (see Figure 1), on which about 32'000 optical
 43 modules are mounted with a pitch of about 1.5 m.
 44 The size of the photodetector needs to be chosen such
 45 that the detectors cover about 8% of the total surface.

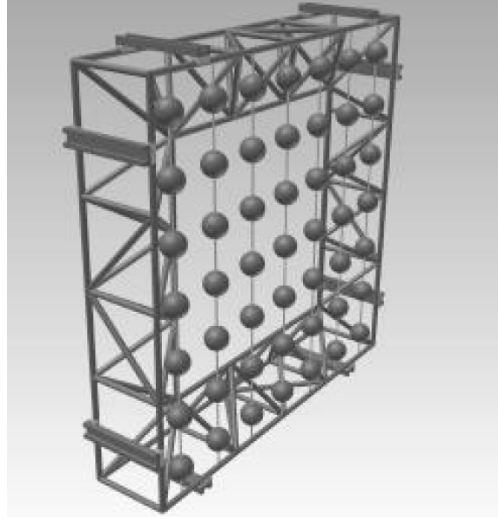


Figure 1: Representation of a mechanical module of 10×10 m² size with 49 Optical Modules.

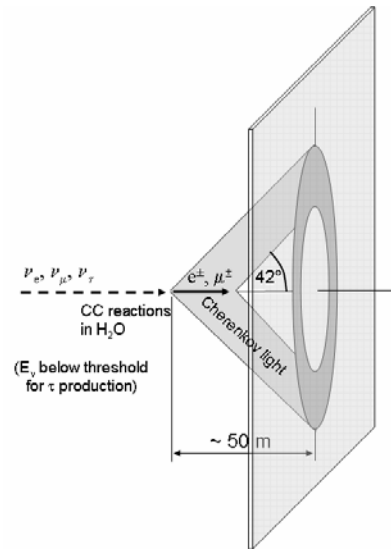


Figure 2: Detection principle of electron and muon neutrinos with a planar water Cherenkov detector (not to scale).

1 As illustrated in Figure 1, this photosensitive wall 43
 2 intercepts the Cherenkov light cone produced by the
 3 charged leptons produced in CC reactions of ν_μ and 44
 4 ν_e . Muon and electron events can be unambiguously 45
 5 distinguished by analyzing the hit distribution on the 46
 6 grid, exploiting characteristic differences of electron 47
 7 and muon interactions in water (shower formation, 48
 8 multiple scattering). The typical Cherenkov ring 49
 9 width is about 3 m, driven by the length of the 50
 10 electron shower and the muon absorption length in 51
 11 water. The light transmission of sea water is limited 52
 12 to the wavelength range $300 < \lambda < 600$ nm with a
 13 peak absorption length $\lambda_{\text{abs}} \approx 55$ m around $\lambda = 450$
 14 nm. The mean value $\langle \lambda_{\text{abs}} \rangle$ in this wavelength range
 15 is about 20 m, which defines together with the grid's
 16 extension a fiducial active detector mass of about 1.5
 17 Mt.

18 2. Photodetector requirements

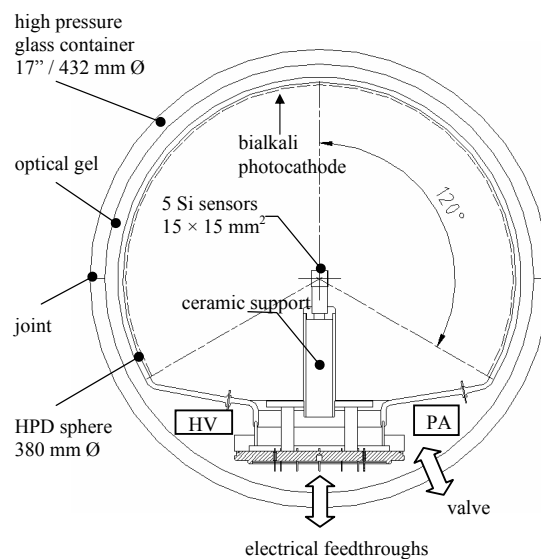
19 The design of the Optical Module is driven by the
 20 experimental requirements and the special
 21 environmental conditions:

- 22 • efficient light detection in the wavelength range
 23 300 - 550 nm;
- 24 • maximal surface and angular acceptance;
- 25 • sensitivity to single photoelectrons;
- 26 • timing resolution ~ 2 ns (TTS + electronics);
- 27 • dark count rate per module < 1 MHz ;
- 28 • operation in sea water at a depth of > 1000 m.

29 Driven by these specifications, but also by
 30 considerations of cost, we embarked on a concept of
 31 an Optical Module which consists of a large, almost
 32 spherical, Hybrid Photon Detector (HPD), inserted in
 33 a spherical glass container which withstands high
 34 pressure. The pressure sphere houses the supplies for
 35 the HV and LV power and the front-end electronics. 59
 36 The detector must provide amplitude information; 60
 37 spatial resolution is not required though. We have
 38 chosen the HPD technology [3] rather than a 61
 39 conventional photomultiplier tube because it provides
 40 very clean signal characteristics and uniform
 41 collection efficiency for even large angles of photon
 42 incidence. 62
 63
 64
 65

3. Concept of a large spherical HPD

Our HPD design is schematically shown in Figure 3.
 It is based on a spherical envelope of borosilicate
 glass of 380 mm outer diameter (wall thickness about
 5 mm). The bottom part of the glass envelope is
 sealed by a metallic baseplate, which supports the
 silicon sensor (see below) and is equipped with
 electrical feedthroughs. A semi-transparent bialkali
 photocathode (quantum efficiency $\sim 25\%$ at 400 nm)
 is best suited for the near-UV and visible wavelength
 range. It covers the inner glass surface down to the



contact electrode which is evaporated on the glass
 surface. The photoelectrons are accelerated in the
 radial electric field between the cathode and the
 silicon anode ($E \sim 1/r^2$).

Figure 3: Schematic view of an optical module based on a spherical HPD

Electrostatic simulations² predict a uniform angular
 acceptance of up to 120° with a transit time spread
 (TTS) below 1 ns. The strongly increasing field leads
 to a focusing effect towards the anode, which reduces
 the point spread originating from the angular spread

² SIMION 3D™. www.simion.com

1 of the electrons at the photocathode. The 50
 2 photocathode is maintained at negative high voltage 51
 3 ($U_C = -20$ kV), while the Si sensor is grounded. The 52
 4 charge gain of the detector is given by the number of 53
 5 electron-hole pairs, which are produced when a 54
 6 photoelectron is stopped in the Si sensor: $G = e \cdot U_C /$ 55
 7 $3.6 \text{ eV} \approx 5000$. The dissipative nature of this gain 56
 8 mechanism leads to a well defined signal with 57
 9 fluctuations generally below the pedestal noise of the 58
 10 readout electronics (see below) and allows for 59
 11 photoelectron counting up to at least five 60
 12 photoelectrons. The large angular coverage is 61
 13 achieved by arranging the anode as five individual 62
 14 silicon sensors of $15 \times 15 \text{ mm}^2$ size, mounted edge- 63
 15 to-edge on a ceramic support cube. The bottom face 64
 16 of the cube sits on an insulated cylinder which is 65
 17 mounted on the baseplate. The cube is surrounded by 66
 18 a round field cage of about 30 mm diameter, which is 67
 19 largely transparent to the photoelectrons. Its rôle is to 68
 20 reduce the electric field gradient in the vicinity of the 69
 21 silicon sensor to values which exclude electric
 22 discharges from the silicon surfaces. In the
 23 simulation the effect of the earth magnetic field (0.5 70
 24 Gauss) on the electron optics is found to be
 25 negligible, a behaviour which was experimentally 71
 26 demonstrated for the conceptionally similar Quasar 72
 27 tubes used in the Lake Baikal experiment [4]. 73
 28 74

29 **The high-pressure container** 75

30 The HPD is housed in a standardized high-pressure 76
 31 glass container as used by the fishing industry. The 77
 32 380 mm HPD fits in a 17-inch container with a gap of 78
 33 1 cm. The lower part of the container provides 79
 34 sufficient space for a compact HV supply, readout 80
 35 and calibration electronics. Industrial pressure and 81
 36 sea-water proof feedthroughs permit electrical 82
 37 supply, control and readout of the Optical Module. 83
 38 The optical and mechanical contact between the HPD 84
 39 and the container is ensured by an optical gel with 85
 40 matched refractive index (the gel also diminishes the 86
 41 vacuum volume, thus reducing the shock wave in 87
 42 water generated by an imploding Optical Module). 88
 43 89

44 **The readout electronics** 90

45 The relatively small signal amplitude ($5000 e^- \approx 1 \text{ fC}$) 91
 46 and the required timing precision ($\sim 2 \text{ ns}$) call for a 92
 47 custom designed low noise front-end, possibly 93
 48 followed by a pulse shape digitization unit. We aim 94
 49 for a signal-to-noise ratio of at least 10 for single 95

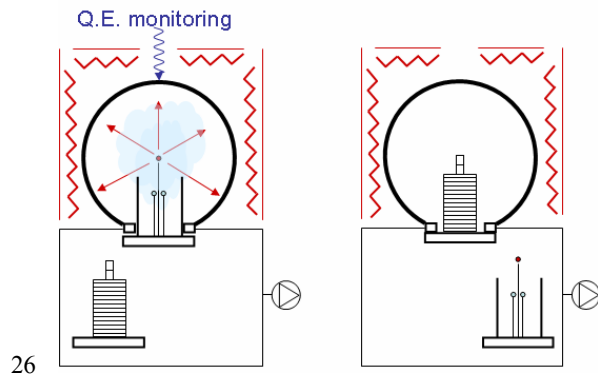
photoelectrons, i.e. the pedestal noise must not
 exceed $500 e^-$ (RMS) and the shaping time of the
 filter/shaper circuit should be of the order 20 ns. A
 front-end with 20 ns shaping time is able to achieve
 noise levels of the order $60\text{-}70 e^-/\text{pF}$. The above-
 mentioned silicon sensors of $15 \times 15 \text{ mm}^2$ (80 pF) are
 therefore segmented in 9 cells such that the capacity
 per cell drops well below 10 pF each. All cells are
 read out by a single chip. Waveform digitization is
 performed at a rate of about 300 MHz.

An alternative approach is to equip the HPD with an
 avalanche silicon diode, commonly used as avalanche
 photodiode (APD). This leads to a conveniently large
 signal amplitude ($\sim 10^5 e^-$), as the HPD
 'bombardment' gain is augmented by the avalanche
 gain. However, the specific detector capacitance of
 avalanche diodes ($300\text{-}1500 \text{ pF}/\text{cm}^2$) and the non-
 availability of large diodes ($> 5 \times 5 \text{ mm}^2$) pose
 limitations, which may be incompatible with a large
 size and acceptance HPD.

4. Fabrication of a large spherical HPD

The large quantity of photodetectors required for a
 neutrino experiment calls for an optimized cost
 efficient industrial production. The standard method
 to produce large hemispherical photomultiplier tubes
 is internal photocathode processing. The phototube is
 pumped through a small glass pumping stud, while
 the tube is vacuum baked, and the photocathode is
 processed by heating the small sources (e.g. Sb, K,
 Cs) which remain inside the tube. The tube is sealed
 after processing by a hot glass seal. An internal
 processing method leads to short turn-around cycles
 as only the tube volume needs to be pumped and
 baked. The tube with all its internal structures is
 exposed to the vapor of the alkali metals, which in
 contrast to Sb spread out over the whole tube volume.
 In a HPD with its characteristic high electric fields,
 the presence of the alkali metals, particularly Cs
 which is known to lower the work function of metals,
 can seriously compromise the capability of a tube to
 achieve the design high voltage. Sparking and
 sustained discharges well below this voltage may be
 a consequence. HPDs are therefore produced in a so-
 called external or transfer process. The entrance
 window or the base plate are kept separate from the
 tube while all components are baked in a vacuum

1 tank The tube is sealed in-situ only after 36
 2 photocathode processing, usually by means of a cold 37
 3 or warm Indium sealing technique. This method
 4 minimizes the ‘pollution’ of the tube and its internal
 5 components with alkali vapors. The use of local 38
 6 heating elements reduces the thermal load of delicate
 7 HPD components like Silicon sensors, ceramic 39
 8 printed circuit boards and readout ASICs. The turn- 40
 9 around time is significantly longer than that of an
 10 internal process, and the set-up is more complex and 42
 11 expensive. While the half-scale prototype discussed 43
 12 below will be fabricated in our existing transfer 44
 13 chamber [5] by an external process, we intend to 45
 14 develop a simple and fast semi-external process for 46
 15 the processing of the large HPD. The process, 47
 16 illustrated in Figure 4, combines elements of the 48
 17 internal and external processes described above. The 49
 18 spherical glass body is connected to a vacuum system 50
 19 and evacuated through the bottom hole. The glass 51
 20 sphere is surrounded by an external oven (at ambient 52
 21 pressure). The evaporation sources are mounted on a 53
 22 movable support which allows to place them in the
 23 sphere centre. After cathode processing the sources
 24 are removed and the sphere is indium-sealed by the
 25 baseplate which carries the silicon



27 Figure 4: Schematic representation of the semi-external process.
 28 Left: Configuration during photocathode processing. Right:
 29 Configuration for tube sealing.

30 sensor arrangement. This process allows to reduce the 54
 31 size of the vacuum tank (short pump down times, 55
 32 little maintenance) and efficiently protects the high
 33 field region from alkali vapor. The bottom flange of
 34 the glass sphere is a challenging component,
 35 currently still under design. It needs to provide a

connection to the vacuum system and allow an in-situ
 sealing with the base-plate.

5. Development of a half-scale prototype

Considerable experience exists at CERN in the
 design and construction of HPDs up to 10 inch
 diameter and with highly pixelized silicon anodes.
 The photocathode evaporation and tube encapsulation
 plant at CERN allows building a prototype HPD of the
 above type with an outer diameter of about 208
 mm (see Figure 5). A large part of the equipment is
 available from previous developments and can be
 adapted with modest effort. The reduced-scale
 prototype allows to verify most of the HPD's
 characteristics, including sensitivity, electrostatics
 and signal properties. A spherical glass envelope,
 which can be sealed with an existing base plate of the
 5-inch Pad HPD [6], is under development at SVT³.
 The anode is formed by 5 non-segmented silicon

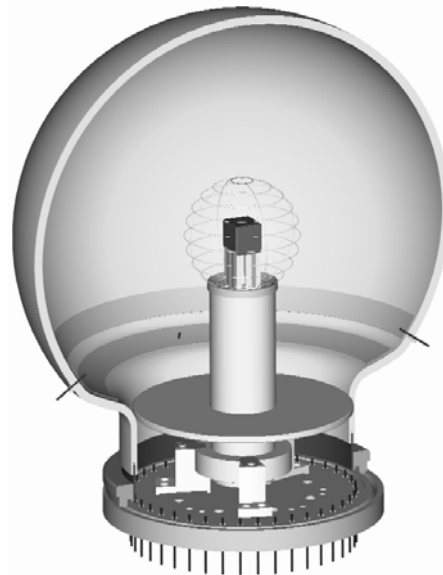


Figure 5: Artistic view of the half-scale prototype tube. The outer
 diameter of the glass sphere is 208 mm.

³ SVT-Vacuum Technology, 91170 Viry-Chatillon, France.

1 sensors of $10 \times 10 \text{ mm}^2$ active size, read out by 15
 2 external electronics. A set of measurements proved
 3 that the required wire length of about 20 cm between 16
 4 the sensor and the external amplifier does not lead to 17
 5 a sizable degradation of the noise performance. It is 18
 6 however clear, that the large capacitance of the non- 19
 7 segmented Si sensor (36 pF) used in this first 20
 8 prototype tube will not allow to achieve the design 21
 9 timing resolution of 2 ns. 22

10 Acknowledgments

11 The authors would like to thank Alan Rudge, 29
 12 Michael Moll and Peter Weilhammer at CERN for 30
 13 clarifying discussions and test measurements on 31
 14 Silicon sensors. 32

33

34

35

36

References

- [1] A. Ball et al., C2GT, Memorandum, CERN-SPSC-2004-025, SPSC-M-723
- [2] G. Acquistapace et al., "The CERN Neutrino Beam to Gran Sasso - Conceptual Technical Design", CERN 98-02 and INFN/AE-98/05. R. Bailey et al., "Addendum to report CERN 98-02", CERN-SL/99-034(DI)
- [3] C. Joram, Hybrid Photodiodes Nucl. Phys. (Proc. Suppl.) B78 (1999) 407.
- [4] B.K. Lubsandorzhiev, Photodetectors of Lake Baikal Neutrino experiment and Tunka Air Cherenkov Array, NIM A 442 (2000) 368-373
- [5] A. Braem et al., Technology of photocathode production, NIM A 502 (2003) 205
- [6] A. Braem et al., Development, Fabrication and Test of a Highly Segmented Hybrid Photodiode, NIM A 478 (2002) 400-403.